

Fig. 2. Variation of  $\beta$  across temperature over BJT corners

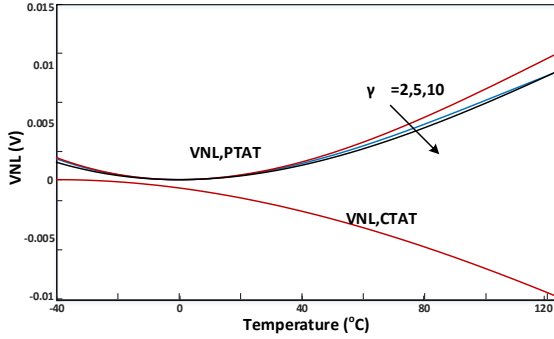


Fig. 3. PTAT and CTAT non-linear terms across temperature

## II. PROPOSED SUB-BANDGAP VOLTAGE REFERENCE

Fig 1 shows the proposed sub 1V bandgap reference circuit which uses the vertical parasitic npn transistors  $Q_1$  and  $Q_2$ . The ratio of the npn is chosen to be 24 in this design. The current mirror M2 and M3 maintain the same current in the BJTs. The operational amplifier reduces the drain-source mismatch of the transistors. It is to be noted that the BJTs will be in active region even if the collector voltage is lower than base voltage by a diode voltage. This results in a sufficient headroom for the current sources  $M_{1-3}$  even at 0.85V supply. The cascodes on these current mirrors are not shown for simplicity. The voltage source  $V_T$  is used to check the start up as discussed in section IV.

The resistor  $R_b$  is used for curvature compensation and is explained in section III. The opamp output is the base-emitter voltage of the bipolar which is CTAT in nature. Unlike other sub 1V bandgap references, this circuit equalizes the collector currents of BJTs. The PTAT current ( $I_c$ ) generated by the difference in the base-emitter voltages of the BJT is given by EQ 1.

$$I_C = \frac{\beta}{\left(1 + \frac{R_b}{R_e}\right) + \beta} \frac{V_T \ln(N)}{R_e} \quad (1)$$

This current is mirrored, converted to voltage using resistors  $R_{1-3}$  and then added to the scaled version of the CTAT

voltage, resulting in a constant reference voltage. The resistors  $R_2$  and  $R_3$  placed at the output of the opamp scales the CTAT voltage. Resistor  $R_1$  converts the mirrored PTAT current by  $M_1$  into voltage, which is added to the scaled CTAT voltage. The sub 1V bandgap voltage is given by EQ 2. Fig 4 shows the schematic of the pmos input-stage opamp. A level-shifter  $M_{15}$  is used to provide headroom to differential pair. The final stage  $M_{10}$  drives the resistance  $R_{2,3}$  in 1. The loop is compensated with zero created by RC.

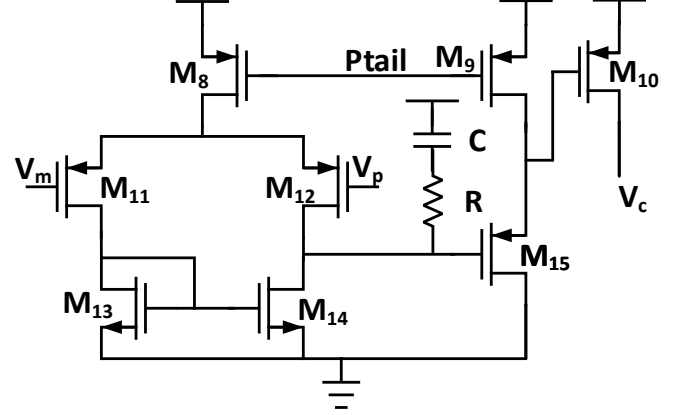


Fig. 4. Schematic of operational amplifier

$$V_{BG} = \left(R_1 + \frac{R_2 R_3}{R_2 + R_3}\right) \frac{\beta}{\left(1 + \frac{R_b}{R_e}\right) + \beta} \frac{V_T \ln(N)}{R_e} + V_{BE1} \frac{R_3}{R_2 + R_3} \quad (2)$$

where  $V_{BE1}$  is given by [4].

$$V_{BE1}(T) = V_{BG} - (V_{BG} - V_{BE10}) \frac{T}{T_0} - (\eta - \alpha) V_T \ln \frac{T}{T_0} \quad (3)$$

where  $\eta$  depends on the bipolar structure and is around 4, and  $\alpha$  is equal to 1 or 0 depending on PTAT or ZTAT current.

$$V_{NL,ctat} = -(\eta - \alpha) V_T \ln \frac{T}{T_0} \quad (4)$$

Expanding the log term of EQ 4 in taylor series and retaining only two terms, we get

$$V_{NL,ctat} = (\eta - \alpha) \frac{k}{q} \left( \frac{T^3}{2T_0^2} - \frac{2T^2}{T_0} + \frac{3T}{2} \right) \quad (5)$$

It is to be noted that the coefficient of quadratic term of temperature in EQ 5 is always negative leading to inverting parabola in the curvature of  $V_{BE1}$ .

The transistor forward gain  $\beta$  increases with temperature [9] as shown in Fig 2  $\beta$  can be represented using a polynomial equation as shown in EQ6.

$$\beta = \beta_0 + \beta_1 T + \beta_2 T^2 \quad (6)$$

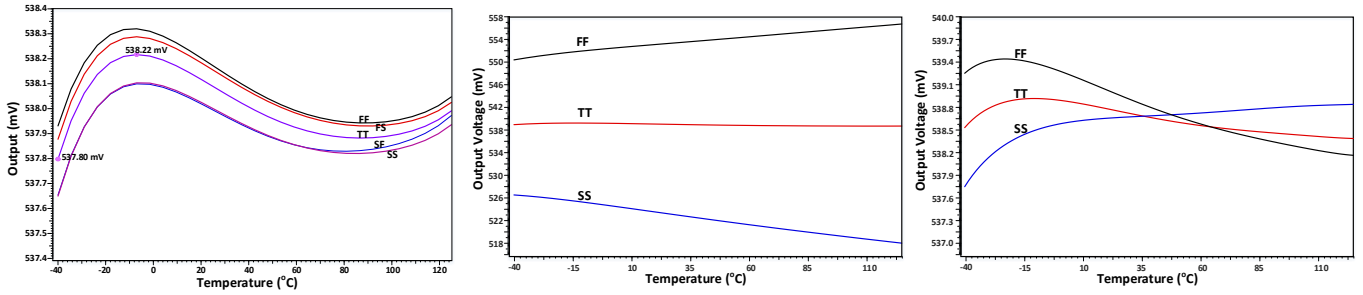


Fig. 5. a) Bandgap voltage with temperature across MOS corners. b) Bandgap voltage with temperature across BJT corners. c) Bandgap voltage with temperature across BJT corners with single point trim

It is to be noted that  $\beta_1$  is always positive. The quadratic coefficient in the PTAT voltage is approximated in EQ 7.  $\beta$  is ignored in the denominator as it is smaller than  $\gamma$ . This is especially true in vertical BJTs in CMOS process. However, quadratic coefficient in PTAT voltage can be adjusted with base and emitter resistances in EQ 7.

$$V_{NL,ptat} = \left( R_1 + \frac{R_2 R_3}{R_2 + R_3} \right) \frac{\beta_1 k \ln(N)}{\gamma q R_e} \quad (7)$$

where  $\gamma$  is  $1 + R_b/R_e$ . The quadratic terms in both PTAT and CTAT voltages has opposite polarity as shown in Fig 3 and they are added in EQ 2 to obtain constant reference voltage.

### III. ERROR SOURCES

The finite output impedance and offset of the current mirrors, operational amplifier offset, the transistor beta mismatch and resistor mismatch are the error sources in the bandgap. The base resistor  $R_b$  will be trimmed at room temperature and all other resistors appear as the ratio in EQ 2. This architecture is insensitive to  $\beta$  variations between transistors as the collector current being matched and the opamp is delivering the base current. The opamp is assumed to have an input-referred offset of  $V_{off}$ , whose standard deviation is given by  $\sigma_{voff}$ . This creates a difference in the current between BJTs to be  $V_{off}/r_o$ , where  $r_o$  is the impedance at the positive terminal of the opamp. This introduces an error in the bandgap voltage, given by EQ 8. The architecture is insensitive to the amplifier offset as it appears in the logarithmic function.

$$\sigma_{e,off} = \left( \frac{\left( R_1 + \frac{R_2 R_3}{R_2 + R_3} \right) \beta V_T}{(R_e + R_b) + R_e \beta I_c r_o} \right)^2 \sigma_{voff}^2 \quad (8)$$

The current mirror mismatch  $M_{2-3}$  causes a current  $gm v_{cmr}$  to flow into Q1, where gm is the transconductance of current source and  $v_{cmr}$  is the offset between current sources with a standard deviation of  $\sigma_{cmr}$ . This creates a similar error to the opamp offset and is given in EQ 9. Let the current mismatch between  $M_{1,3}$  caused by both offset and vds mismatch be represented as  $I_m$  with standard deviation of  $\sigma_m$ . This results in an error as given by EQ 10.

$$\sigma_{e,cmr}^2 = \left( \frac{\left( R_1 + \frac{R_2 R_3}{R_2 + R_3} \right) \beta V_T g_m}{(R_e + R_b) + R_e \beta I_c} \right)^2 \sigma_{cmr}^2 \quad (9)$$

$$\sigma_{e,m}^2 = \sigma_m^2 \left( R_1 + \frac{R_2 R_3}{R_2 + R_3} \right)^2 \quad (10)$$

Since all are uncorrelated random variables, the total error is obtained as

$$\sigma_e^2 = \sigma_{e,off}^2 + \sigma_{e,cmr}^2 + \sigma_{e,m}^2 \quad (11)$$

It is observed from EQ 11, that all error sources except  $\sigma_{e,m}$  are suppressed by the npn gain. Hence in this design the current sources are cascoded and heavily degenerated. However, they are not shown here for simplicity. It is to be noted that the current sources have sufficient headroom as the collector voltage can go below the base by one diode voltage for bipolar.

### IV. SIMULATION RESULTS

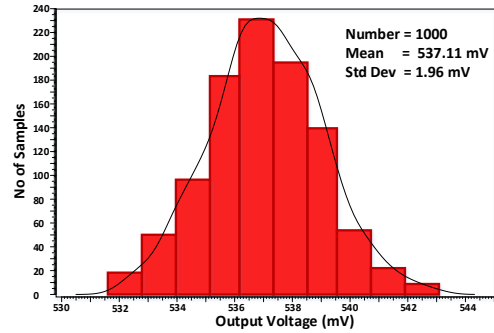


Fig. 6. Monte-Carlo simulation on proposed bandgap

The proposed bandgap reference as shown in Fig 8 was designed and simulated in TSMC 28nm CMOS process and occupies an area of  $77\mu m \times 95\mu m$ . The layout includes all decaps and compensation capacitors used in the design. The bandgap core has the ratio of 24 for noise optimization. This bandgap was simulated across all MOS corners and the reference voltage is plotted with temperature in Fig 5a.

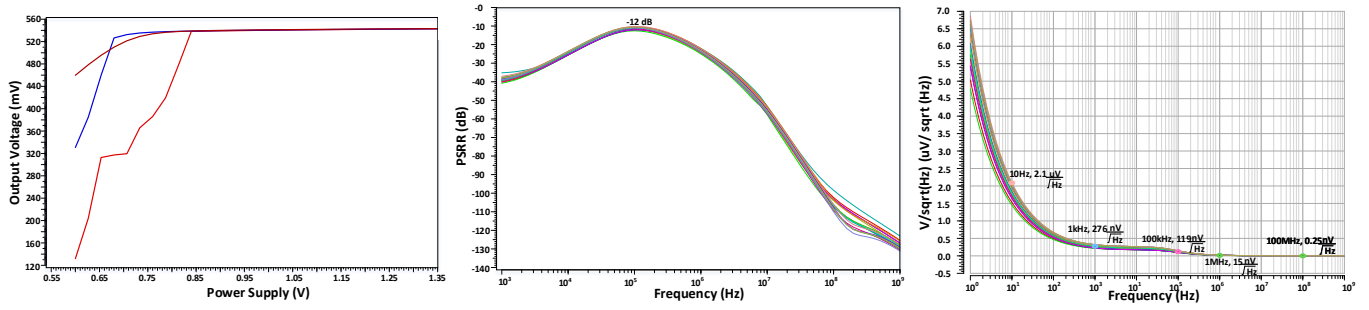


Fig. 7. a)Bandgap voltage with power supply. b)Power Supply Rejection Ratio at bandgap output across corners. c)Noise power spectral density at bandgap output across corners

The bandgap has about  $4.7 \text{ ppm}/^\circ\text{C}$  across temperature in a typical corner. The variation of the reference voltage across corners is about  $0.2\text{mV}$ . The bandgap is simulated across all BJT corners in Fig 5b. The variation of the reference voltage in about 5%. We cross verified this variation against a standard Brokaw [1] architecture. A single point trim at  $R_b$  reduces the worst case accuracy from  $139\text{ppm}/^\circ\text{C}$  to  $12\text{ppm}/^\circ\text{C}$  as shown in Fig 5c. This is attributed to change in the PTAT current and the BJT corner which changes its base emitter voltage. The circuit is simulated across a power supply to see its line regulation as shown in Fig 7a and line sensitivity obtained is  $0.5 \%$  when the supply changes from  $850\text{mV}$  to  $1.35\text{V}$ .

Monte-Carlo simulations were run across 1000 samples to see the effect of mismatches as shown in Fig 6. As explained in section III, only PTAT current mirror  $M_{1,3}$  contributes to a significant part of the mismatch. The mean across 1000 runs is about  $537.1\text{mV}$  with a standard deviation of  $1.96\text{mV}$  which is  $0.36\%$ . The Power Supply Rejection Ratio (PSRR)

at the output is plotted in Fig 7c across all corners and is  $276\text{nV}/\sqrt{\text{Hz}}$  at  $1\text{KHz}$ .

## V. CONCLUSION

A voltage mode sub-1V bandgap reference voltage has been designed in TSMC 28nm CMOS technology with a  $0.85\text{V}$  power supply. This architecture relaxes the opamp offset and flicker noise specifications and doesn't necessitates the use of techniques, such as chopping. Curvature compensation is achieved with the help of the base resistor. The mechanism of curvature-compensation is derived analytically and verified across simulations. Single point trim places the worst case accuracy at  $12\text{ppm}/^\circ\text{C}$ . This circuit also inherently provides PTAT current along with a constant voltage to be used for applications like temperature sensors and oscillators.

## REFERENCES

- [1] A. Brokaw, "A simple three-terminal IC bandgap reference," *IEEE Journal of Solid-State Circuits*, vol. 9, pp. 388–393, Dec. 1974.
- [2] H. Banba, H. Shiga, A. Umezawa, T. Miyaba, T. Tanzawa, S. Atsumi, and K. Sakui, "A CMOS bandgap reference circuit with sub-1-V operation," *IEEE Journal of Solid-State Circuits*, vol. 34, pp. 670–674, May 1999.
- [3] G. Zhu, Y. Yang, and Q. Zhang, "A 4.6-ppm/c High-Order Curvature Compensated Bandgap Reference for BMIC," *IEEE Transactions on Circuits and Systems II: Express Briefs*, vol. 66, pp. 1492–1496, Sep. 2019.
- [4] P. Malcovati, F. Maloberti, C. Focci, and M. Pruzzi, "Curvature-compensated BiCMOS bandgap with 1-V supply voltage," *IEEE Journal of Solid-State Circuits*, vol. 36, no. 7, pp. 1076–1081, Jul. 2001.
- [5] J. Yin, J. Yi, M. K. Law, Y. Ling, M. C. Lee, K. P. Ng, B. Gao, H. C. Luong, A. Bermak, M. Chan, W.-H. Ki, C.-Y. Tsui, and M. Yuen, "A System-on-Chip EPC Gen-2 Passive UHF RFID Tag With Embedded Temperature Sensor," *IEEE Journal of Solid-State Circuits*, pp. 2404–2420, Nov. 2010.
- [6] Sanborn, Keith, D. Ma, and V. Ivanov, "A sub-1-v low-noise bandgap voltage reference," *IEEE Journal of Solid-State Circuits*, vol. 42, no. 11, pp. 2466–2081, Nov. 2007.
- [7] Q. Duan and J. Roh, "A 1.2-V 4.2 ppm/c High-Order Curvature-Compensated CMOS Bandgap Reference," *IEEE Transactions on Circuits and Systems I: Regular Papers*, vol. 62, Mar. 2015.
- [8] R. Nagulapalli, R. K. Palani, and S. Bhagavatula, "A 24.4 ppm/oc voltage mode bandgap reference with a 1.05v supply," *IEEE Transactions on Circuits and Systems II: Express Briefs*, pp. 1–1, 2020.
- [9] S. Hussain, R. C. Jaeger, J. C. Suhling, B. M. Wilamowski, M. C. Hamilton, and P. Gnanachelvi, "Understanding the impact of temperature variations on measurement of stress dependent parameters of bipolar junction transistors," in *Fourteenth Intersociety Conference on Thermal and Thermomechanical Phenomena in Electronic Systems (ITherm)*, May 2014, pp. 1244–1250.

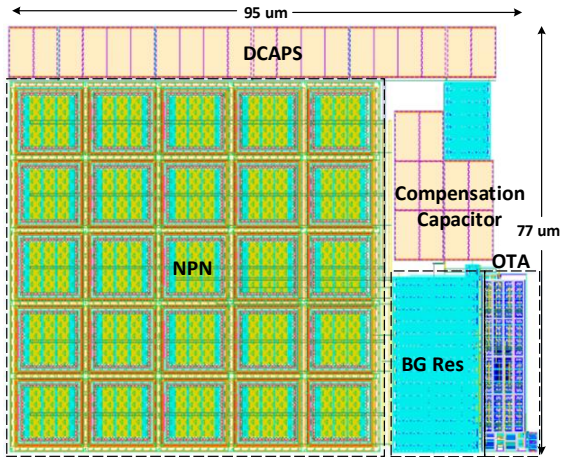


Fig. 8. Layout of the bandgap circuit

was simulated across all corners by injecting a  $1\text{V}$  AC signal at the power supply and the gain at the output reference node was plotted against input frequency. Fig 7b shows that the DC PSRR is  $-40\text{dB}$ . A filter with the resistance of  $100\text{k}\Omega$  and capacitor of  $7.5\text{pF}$  is placed at the bandgap output to limit the maximum PSR to  $-12\text{dB}$ . The noise spectral density